Human Molecular Genetics, 2014, Vol. 23, No. 9 **2339–2352**
doi:10.1093/hmg/ddt627
Advance Access published on December 11, 2013

Recessive and dominant mutations in *COL12A1* cause a novel EDS/myopathy overlap syndrome in humans and mice

Yaqun Zou[1], Daniela Zwolanek[2], Yayoi Izu[3], Shreya Gandhy[1], Gudrun Schreiber[4], Knut Brockmann[5], Marcella Devoto[6,7,8], Zuozhen Tian[9], Ying Hu[1], Guido Veit[3], Markus Meier[10], Jörg Stetefeld[10], Debbie Hicks[11], Volker Straub[11], Nicol C. Voermans[12], David E. Birk[3], Elisabeth R. Barton[9], Manuel Koch[2,*] and Carsten G. Bönnemann[1,*]

[1]Neuromuscular and Neurogenetic Disorders of Childhood Section, National Institute of Neurological Disorders and Stroke, NIH, Bethesda, MD, USA, [2]Medical Faculty, Institute for Dental Research and Oral Musculoskeletal Biology, Center for Molecular Medicine Cologne, Center for Biochemistry, University of Cologne, D-50931 Cologne, Germany, [3]Department of Molecular Pharmacology and Physiology, University of South Florida, Tampa, FL, USA, [4]Clinical Center for Pediatric Neurology, Kassel, Germany, [5]Interdisciplinary Pediatric Center for Children with Developmental Disabilities, University Medical Center, Göttingen, Germany, [6]Division of Human Genetics and Department of Pediatrics, The Children's Hospital of Philadelphia, Philadelphia, PA, USA, [7]Department of Biostatistics and Epidemiology, Perelman School of Medicine, University of Pennsylvania, Philadelphia, PA, USA, [8]Department of Molecular Medicine, University La Sapienza, Rome, Italy, [9]Department of Anatomy and Cell Biology, School of Dental Medicine, University of Pennsylvania, PA, USA, [10]Department of Chemistry, Microbiology, Biochemistry and Medical Genetics, University of Manitoba, Canada, [11]Institute of Genetic Medicine, Newcastle University, Newcastle upon Tyne, UK and [12]Department of Neurology, Radboud University Nijmegen Medical Centre, Nijmegen, The Netherlands

Received October 1, 2013; Revised December 3, 2013; Accepted December 9, 2013

Collagen VI-related myopathies are disorders of connective tissue presenting with an overlap phenotype combining clinical involvement from the muscle and from the connective tissue. Not all patients displaying related overlap phenotypes between muscle and connective tissue have mutations in collagen VI. Here, we report a homozygous recessive loss of function mutation and a *de novo* dominant mutation in collagen XII (COL12A1) as underlying a novel overlap syndrome involving muscle and connective tissue. Two siblings homozygous for a loss of function mutation showed widespread joint hyperlaxity combined with weakness precluding independent ambulation, while the patient with the *de novo* missense mutation was more mildly affected, showing improvement including the acquisition of walking. A mouse model with inactivation of the *Col12a1* gene showed decreased grip strength, a delay in fiber-type transition and a deficiency in passive force generation while the muscle seems more resistant to eccentric contraction induced force drop, indicating a role for a matrix-based passive force-transducing elastic element in the generation of the weakness. This new muscle connective tissue overlap syndrome expands on the emerging importance of the muscle extracellular matrix in the pathogenesis of muscle disease.

*To whom correspondence should be addressed at: Neuromuscular and Neurogenetic Disorders of Childhood Section, NINDS/NIH, Porter Neuroscience Research Center, 35 Convent Drive, Bldg 35, Room 2A-116, Bethesda, MD 20892-3705, USA. Email: carsten.bonnemann@nih.gov (C.G.B.); Institute for Dental Research and Oral Musculoskeletal Biology, Medical Faculty, University of Cologne, Joseph-Stelzmann-Str. 52, 50931 Köln. Email: manuel.koch@uni-koeln.de (M.K.)

INTRODUCTION

Mutations in three genes encoding for collagen type VI (COL6A1, COL6A2 and COL6A3) have been found to underlie a spectrum of myopathies ranging from the severe congenital Ullrich disease via intermediate phenotypes to the milder Bethlem myopathy (1). Characteristically, patients affected by collagen VI-related myopathies show clinical features of both a myopathy as well as of a disorder of connective tissue. The connective tissue involvement is reminiscent of that seen in the Ehlers-Danlos syndromes (EDS) in that there is a characteristic distal hypermobility of joints, but there are also significant and progressive large joint contractures, which are not typically seen in the EDS (1,2). Patients with the typical Ullrich presentation of collagen VI-related myopathies are very hypotonic at birth with striking hypermobility of the joints together with soft skin in the hand and feet and a prominent calcaneus. There may be concomitant joint contractures at birth, including hip and knee contractures as well as kyphoscoliosis and torticollis. The contractures have a tendency to worsen over time. At the same time, there is a progressive myopathy that evolves from an initially mostly atrophic histological phenotype (3,4) to a more and more dystrophic appearing histological phenotype along with progressive loss of strength.

Collagen type VI is widely expressed in many extracellular matrices. In muscle, collagen VI is closely associated with the muscle fiber basement membrane, while its cells of origin are muscle interstitial fibroblasts (5,6). Collagen type VI is also prominently expressed in tendon and skin, as the basis for the dual nature of the clinical phenotype as both a disorder of muscle as well as of connective tissue. In the majority of patients, a typical clinical phenotype of Ullrich disease is caused by mutations in the collagen VI genes, supported by collagen VI immunocytochemical studies on fibroblasts and muscle biopsy specimen, which will show a clearly reduced amount and/or abnormal localization of collagen VI with respect to the basement membrane (1). However, there are also patients with clinical features reminiscent of Ullrich congenital muscular dystrophy with normal collagen VI immunocytochemical and genetic studies for whom the primary defect has remained elusive.

Collagen XII is a member of the family of fibril-associated collagens with interrupted triple helical domains (FACIT) (7). Collagen XII is a homotrimer consisting of three alpha1 (XII) polypeptide chains, which are subdivided into two collagen triple-helical domains (referred to as COL1 and COL2) and three non-triple-helical domains (NC1, NC2 and NC3). The large globular N-terminal NC3 domain consists of two to four von Willebrand factor type A domains, several fibronectin type III repeats and a thrombospondin N-terminal domain. Collagen XII is found most commonly in tissues also containing collagen I fibrils, where by ultrastructure it localizes near the surface of the collagen I fibrils (7). Collagen XII is highly expressed in tissues that have mechanical functions, where it has been suggested that it functions as a modulator of biomechanical properties (8–10) by bridging collagen I-containing fibrils to other extracellular matrix components, such as decorin and fibromodulin (11,12) and tenascin-X (13). Similar to collagen VI (5), collagen XII is not expressed by muscle cell but likely also by interstitial fibroblasts (14). In mammalian and avian species, there are two splice variants of the collagen XII alpha1 chain: collagen XIIA (long form) and collagen XIIB (short form). Collagen XIIA is the predominant form during the early development of the embryo, while at later developmental stages collagen XIIB becomes the major form while the XIIA form continues to be expressed in only a few dense connective tissue such as bone, tendon, ligament, dermis, cornea, blood vessel wall and meninges (14–17). In chicken metatarsal tendon, even though collagen XII is present in all stages of development, its expression changes from encompassing the entire tendon while the tendon is immature and fascicles are not well developed, to just the interfacial matrix (endotendineum) associated with developing fascicles. This indicates that collagen XII may help integrate the developing tendon matrices and fascicles into a functional unit (7). Interestingly, a similar role has been suggested for collagen VI based on work in a mouse model with collagen VI deficiency due a Col6a3 mutation (18). In zebra fish, collagen XII is ubiquitously expressed in the connective tissue sheaths that encase the tissues and organs of the body (19).

Here, we report the identification of mutations in human collagen type XII in patients with a striking overlap phenotype combining a joint hypermobility syndrome with a myopathy. In two families, we find recessively as well as dominantly acting mutations with the recessive complete loss of function causing the most severe clinical phenotype, reminiscent of Ullrich disease but with clinically significant differences. We also demonstrate that loss of collagen XII in the mouse is associated with evidence for muscle weakness as well as changes in fiber-type composition in the muscle. We find that the muscle shows changed elasticity and therefore decreased passive force generation rather than a loss in active-specific force. We speculate that this change in matrix elasticity causes a functional unloading of the muscle and decreased force transmission.

RESULTS

Clinical findings

Family A: the two affected boys in the first family were born to consanguineous parents of Turkish descent. The first patient (patient A1, Fig. 1A) was born after an uncomplicated pregnancy with a birth weight of 2660 g. He was noted to be profoundly weak with barely antigravity strength at birth and strikingly hypermobile distal joints while at the same time showing moderate more proximal contractures as well as kyphoscoliosis. In addition, he had mild facial weakness, a high arched palate and absent deep tendon reflexes. Because of poor feeding and swallowing, a percutaneous G-tube was inserted before 2 years of age. Documented night-time hypoventilation resulted in the initiation of non-invasive night-time ventilation before 3 years of age. Motor development continued to be severely delayed. He was eventually able to get from a lying to a sitting position, but not to standing or walking, requiring a power wheelchair for mobility. His initial kyphosis developed into progressive scoliosis, requiring spinal fixation surgery at 9 years of age.

His younger brother (patient A2, Fig. 1C) had very similar clinical findings at birth, presenting with a combination of weakness with significant distal hyperlaxity and milder proximal contractures. He also was able to get to a sitting position, but not to standing or walking.

Creatine kinase values in both boys were normal, whereas muscle biopsy was consistent with a myopathy with variability

Figure 1. Clinical presentations: weakness, distal joint hyperlaxity with co-existing knee contractures and kyphoscoliosis were present in patient A1 (**A**) and his younger brother A2 (**C**). Lax hands and feet and stooped posture were present in patient B at 2 years of age (**B**), improved posture was evident at age 3 years (**D**).

in fiber diameter, but without any overt signs of degeneration or regeneration. Nerve conduction velocities were normal. Muscle biopsy in patient A1 revealed variability in fiber diameter but no evidence for active degeneration or regeneration.

There was one unaffected brother with normal motor development. Both parents were noted to have delayed early motor development acquiring the ability to walk after 2 years of age, but eventually showing normal strength. Of note was that in the extended family, a number of family members were noted to have died in early childhood, apparently with similar presentations to our patients. Unfortunately, we were unable to get more information or DNA on these family members in Turkey.

Family B: this boy was identified by screening dermal fibroblast cultures from patients with weakness and joint hyperlaxity and in whom collagen VI had been found to be normal for abnormalities of collagen XII by immunocytochemistry. He is the first child of clinically unaffected non-consanguineous parents. Hypotonia, proximal joint contractures and distal joint hyperlaxity were noted during the first year of life. Motor development was delayed and he started to walk shortly before his second birthday. He was unable to run and initially walked with a stooped posture (Fig. 1B). He continued to improve over the next year, and was able to walk with a less stooped posture by the end of the third year of life and from there has continued to improve (Fig. 1D). Knee contractures resolved completely and elbow contractures improved gradually. There was mild kyphosis but no scoliosis. Language development and cognition were normal. Muscle ultrasound of the thigh showed mild diffuse increase in echogenicity without fasciculations. Nerve conduction studies were normal. Muscle biopsy showed mild variability in fiber diameter without evidence for degeneration or regeneration, consistent with a mild myopathy.

Haplotype and mutation analysis

Haplotype analysis for shared regions of homozygosity was performed in family A, and included the parents, the two affected boys and the unaffected sibling. The only region of homozygosity shared between the two affected brothers but not the unaffected

sibling was on chromosome 6, between SNPs rs1158058 and rs1665914 (chr6: 71 783 260–107 436 099) containing COL 12A1 as a logical candidate. Mutation analysis was performed on patient dermal fibroblast derived cDNA. Gel electrophoresis of the PCR fragments revealed a smaller fragment compared with a control, sequencing of the fragment showed skipping of exon 50 in the patient cDNA. Analysis of genomic DNA revealed a homozygous mutation (NM 004370 c. 8006+1G>A) of the splice donor site of intron 50, as the basis for the skipping of exon 50. The resulting transcript is out of frame, reaching a stop codon in exon 51 (NP_004361 p. 2567 Asp>PhefsX2) (Fig. 2A). This mutation is not reported as a variant in dbSNP http://www.ncbi.nlm.nih.gov/projects/SNP), or the 1000 Genomes project (www.1000genomes.org). The predicted premature stop leads to a truncation of the protein upstream of the short collagenous domains. It would be expected that the resulting predicted protein would be expected to not be able to assemble due to the lack of its triple helical domains. Both parents were found to be carriers.

The mutation in patient B (NM004370 c. 7167 T>C; NP004361 p. Ile2334Thr) is situated directly adjacent to a predicted MIDAS domain (DXSXSX) in the last VWA domain of the NC3 domain (Fig. 2B). This highly conserved sequence responsible for coordination of bivalent cations and mediation of e.g. integrin–collagen interactions (20–22). Molecular modeling of the point mutation that changes Ile156 to a b-branched polar threonine residue shows that is located in the L1-loop segment flanking the MIDAS motif (Fig. 2C and D). The hydroxyl moiety of Thr156 is in hydrogen bonding distance to interact with Asp151, one of the two aspartate side chains involved in metal coordination. In addition, Asp151 is also stabilizing the first serine residue (Ser153) in the DXSXS motif

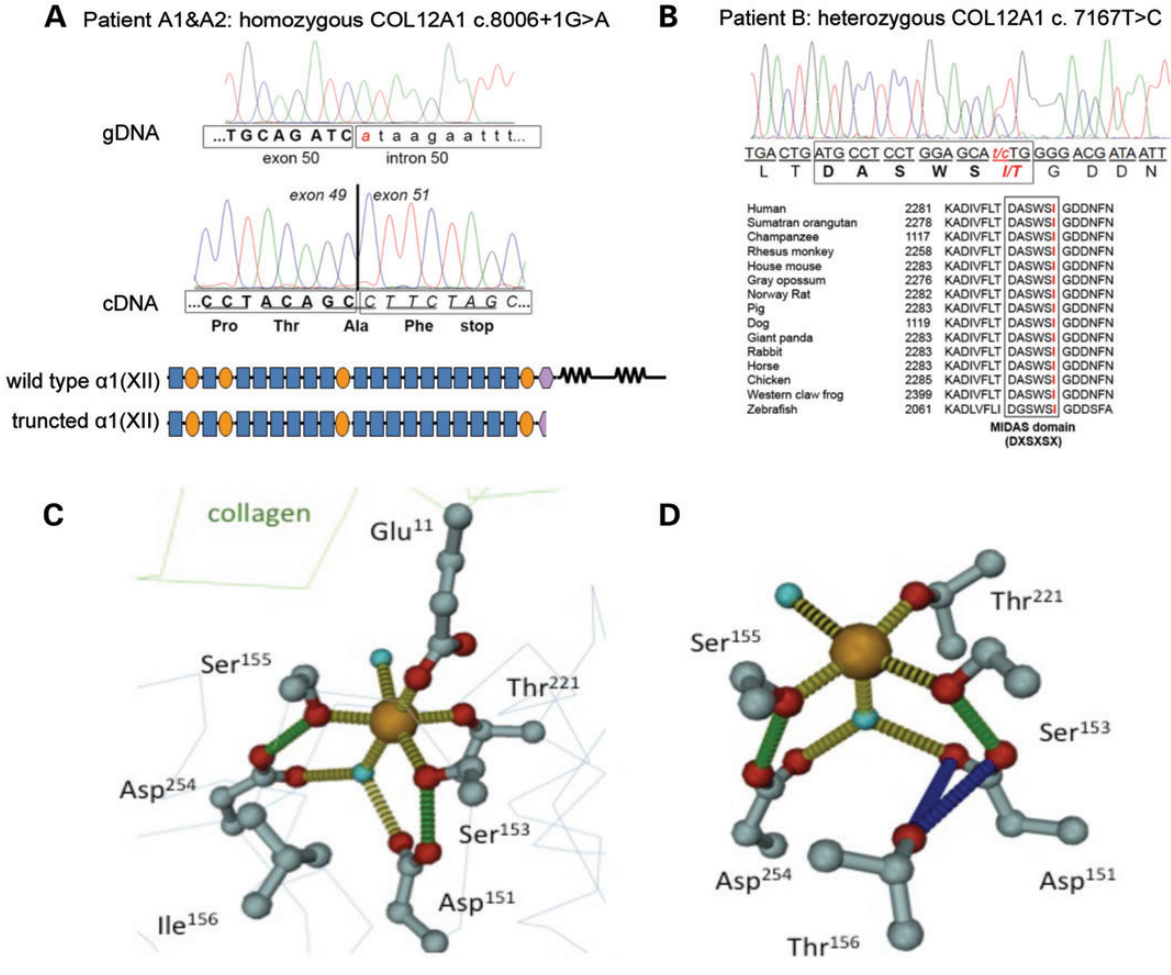

Figure 2. COL12A1 mutation in family A and patient B. In family A (patient A1 and A2), a homozygous splicing mutation (NM004370 c. 8006+1G>A) causes out-of-frame skipping of exon 50, resulting in a premature stop codon in exon 51 in the shifted reading frame, translating into a truncated protein without collagen domains (**A**). In patient B, the *de novo* heterozygous missense mutation (NM004370 c. 7167 T>C; NP_004361 p. Ile2334Thr) is located directly adjacent to a predicted MIDAS motif (DXSXSX) in the last VWA domain, which is conserved from zebrafish to human (**B**). Molecular modeling of the MIDAS motif in a wild-type VWA domain and predicted mutant VWA domain in patient B (**C** and **D**). The octahedral coordination of the metallic ligand (orange ball) is shown as yellow dotted line, with both water molecules as turquoise spheres. Glu11 from the collagen-binding partner is completing the binding sphere. Green-dotted lines symbolize intramolecular hydrogen binds between both, Asp151 (L1) and Asp254 (L3) with Ser153 and Ser155, respectively. The point mutation of Ile156Thr causes a destabilizing of the water-mediated metal chelating via Asp151 and the direct binding via Ser153. The hydroxyl group of the threonine side chain can establish strong polar interactions with the carboxylic moiety of Asp151, pulling it away from the metal. In addition, Thr156 can establish polar interactions with both carbonyl oxygen of Asp151 and Ser153 (data not shown).

that directly binds the metal through the hydroxyl oxygen. As a consequence of the Thr156 insertion, the octahedral coordination sphere of the metal binding site is disrupted and most probably the binding affinity is reduced.

Human fibroblast culture and muscle biopsy analysis

Family A: immunocytochemical analysis of dermal fibroblast cultures derived from patient A1 with a collagen XII specific antibody [KR75 (23)] without the addition of triton X-100 showed a complete absence of collagen XII immunoreactive matrix deposition (Fig. 3A). In contrast, immunocytochemical analysis of control fibroblasts revealed a finely spun extracellular matrix in the culture (Fig. 3C). With the addition of triton X-100 to visualize intracellular immunoreactive material, also there was intracellular collagen XII immunoreactive material visible in the control cells (Fig. 3F) but not in the cells from the patient (Fig. 3D). Immunocytochemical analysis of the same cultures using collagen VI-specific antibody (MAB1944, Millipore, Temecula, CA, USA) showed that there was no difference in the collagen VI between patient (Fig. 3G) and control (Fig. 3I). Immunoblotting analysis with collagen XII-specific antibody [KR75 (23)] showed that there was no collagen XII in patient A1 fibroblasts but about the same amount of collagen VI as in normal control fibroblast (Fig. 3J). The fibronectin matrix formation as assessed by immuocytochemistry using a fibronectin-specific antibody was also normal in the fibroblast culture of patient A1 (data not shown). Relative quantitative PCR analysis showed COL12A1 transcript level in fibroblasts from patient A1 to be only 3% of the average COL12A1 transcript level in normal control

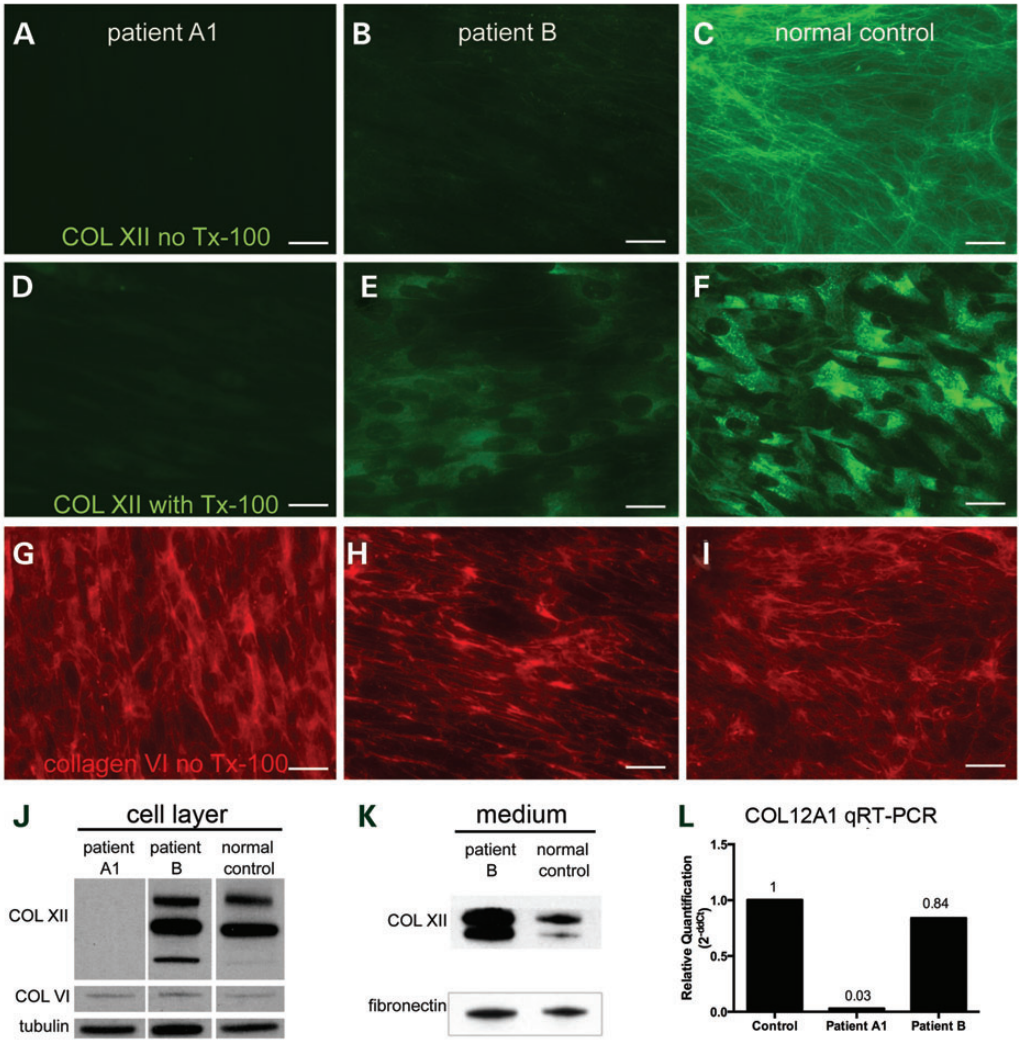

Figure 3. Abnormal collagen XII expression in patient derived fibroblasts: both extracellular (**A**) and intracellular (**D**, with Tx-100) collagen XII immunoreactivity were completely absent in fibroblasts derived from patient A1; in fibroblasts derived from patient B, the collagen XII matrix (**B**) was significantly reduced, but intracellular collagen XII was still present (**E**, with Tx-100). The collagen VI matrix was well preserved in fibroblasts from patient A1 (**G**) and patient B (**H**). Fibroblasts derived from a normal control were used as staining control for collagen XII [extracellular (**C**), intracellular (**F**, with Tx-100)] and collagen VI (**I**). As shown by immunoblotting, collagen XII was absent in cell layer (**J**) of fibroblast culture of patient A1; collagen XII was present in the cell layer (J) and present and increased in the conditioned medium (**K**) from the fibroblast culture of patient B. In both patients, collagen VI from cell layer (J) and fibronectin from conditioned medium (K) were unchanged. (**L**) Relative quantitative RT-PCR revealed the COL12A1 transcription level in patient A1 fibroblasts to be only 3% of that in normal control fibroblasts (average results from eight different normal control cell line), while the COL12A1 transcription level appeared unchanged in patient B fibroblasts comparing with that in normal control fibroblasts (L). Scale bar = 25 μm.

fibroblasts (average of eight normal control fibroblasts), indicating premature decay of the mutant message, presumably on the basis of nonsense-mediated decay triggered by the new stop codon introduced by the out of frame skipping of exon 50 (Fig. 3L).

Immunohistochemical analysis of a muscle biopsy specimen from patient A1 showed normal staining for collagen VI (Fig. 4D) with normal localization in the basement membrane (data not shown). Collagen XII immunoreactivity in a normal muscle biopsy was strongly positive in the perimysium, and less strongly in the endomysium (Fig. 4C), but in contrast to collagen VI it did not overlap with the basement membrane (Fig. 4G–I). In the muscle biopsy from patient A1, there was complete absence of collagen XII immunoreactivity (Fig. 4A), compared with normal control specimen (Fig. 4C). Laminin gamma1 as a basement membrane marker was also normally preserved in both patient muscle biopsies (data not shown).

Family B: immunocytochemical analysis of dermal fibroblasts showed prominent reduction of the collagen XII matrix in the culture derived from patient B (Fig. 3B) compared with the normal control culture (Fig. 3C). With the addition of triton X-100 to visualize intracellular immunoreactive material, the patient's fibroblasts (Fig. 3E) showed similar intracellular collagen XII reactive material as seen in the normal control (Fig. 3F). The patient-derived fibroblasts produced a normal appearing collagen VI matrix (Fig. 3H). Immunoblotting analysis showed collagen XII existed in both cell layer and conditioned medium of patient fibroblast, with some apparent increase in the medium of the patient fibroblasts (Fig. 3J and K). Relative quantitative PCR result showed that the COL12A1 transcript level in fibroblasts from patient B was 84% of the average COL12A1 transcript level in normal control fibroblasts (average of eight normal control fibroblasts) (Fig. 3L). Immunohistochemical analysis of the muscle biopsy from the patient B showed collagen XII immunoreactivity at the endomysium and perimysium with some reduction in particular in endomysium (Fig. 4B), while collagen VI immunoreactivity seems preserved (Fig. 4E).

Phenotypical analysis in *Col12a1*$^{-/-}$ mice

The *Col12a1*$^{-/-}$ mouse model was generated previously by targeted deletion of exons 2–5 (24) and had been analyzed for abnormalities of bone formation without analysis of their neuromuscular phenotype. Although the mice appeared to behave normally, there was evidence for the presence of weakness, as evidenced by decreased hindlimb splaying when on tail suspension (Fig. 5A and B) and also significantly decreased grip strength compared with wild-type controls (Fig. 5C and D). X ray analysis of the

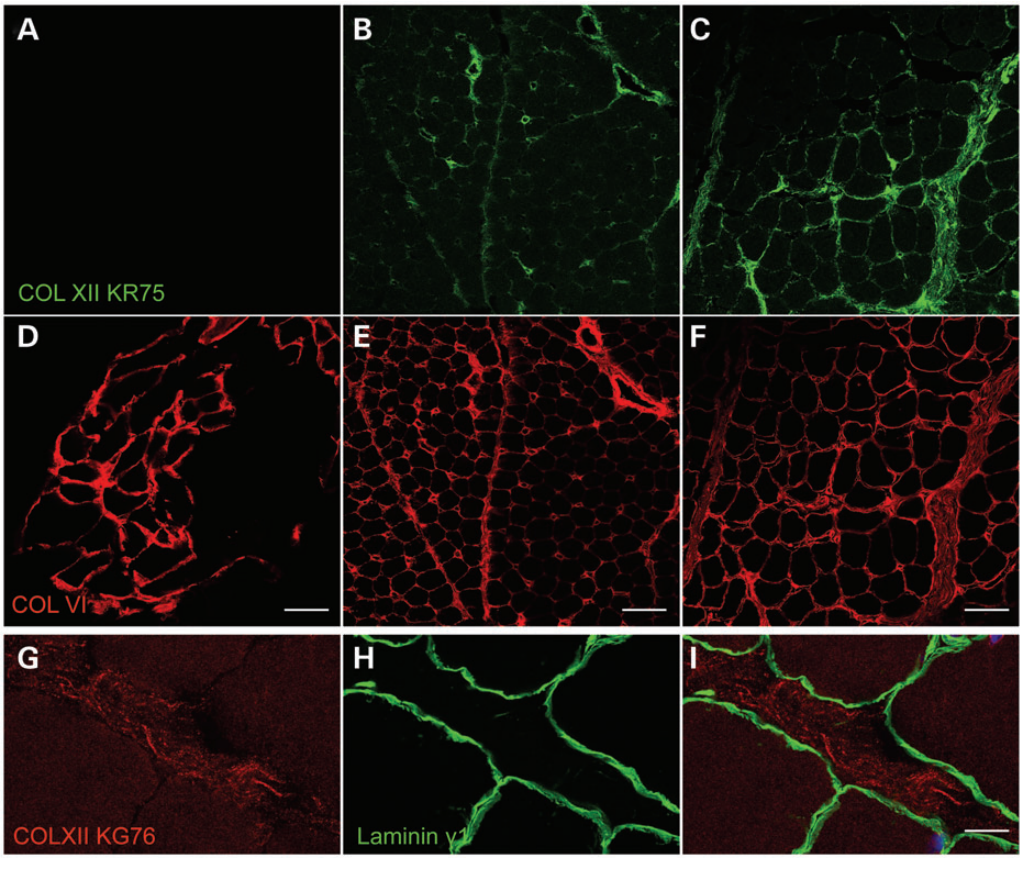

Figure 4. Collagen XII expression and localization in patient muscle biopsies and normal control: in normal control muscle, collagen XII was observed at endomysium and perimysium (**C**). Although it had a similar general localization compared with collagen VI (**F**), collagen XII (**G**) did not partially overlap with muscle fiber basement membrane labeled with laminin γ1-specific antibody (**H** and **I**); in patient A1, collagen XII was completely absent (**A**); in patient B, collagen XII was observed in the endomysium and perimysium, but relatively reduced especially in the endomysium (**B**). In contrast, collagen VI was well preserved at endomysium in both patient A1 (**D**) and patient B (**E**). Scale bar = 50 μm (A–F), = 10 μm (G–I).

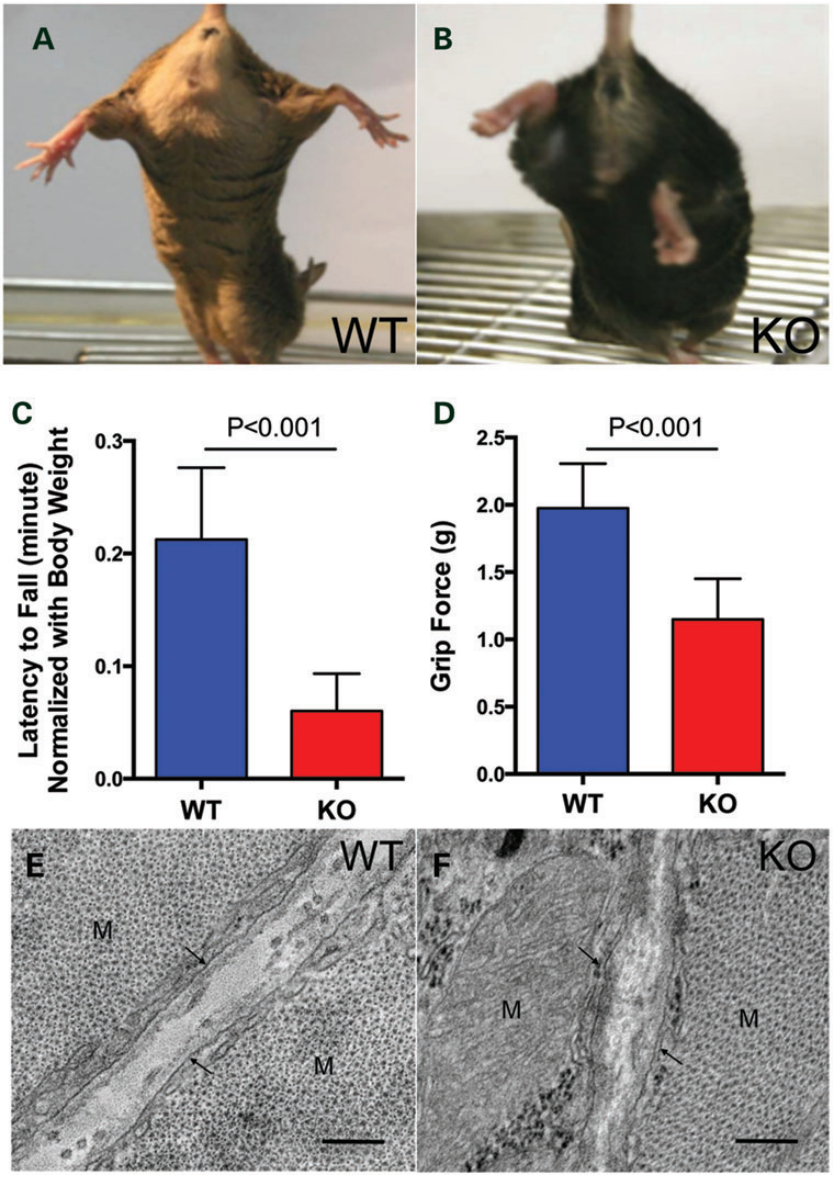

Figure 5. Muscle weakness and altered muscle ultrastructure in Col12a1$^{-/-}$ mice: in the hind limb splay test, Col12a1 knockout mice (**B**) showed decreased hind limb splaying compared with wild-type mice (**A**); as shown in both the hanging test (**C**) and the machine test (**D**), grip strength was significantly reduced in Col12a1 knockout mice. Transmission electron microscopy images of myocytes (M) at P30: In the wild-type collagen fibrils were localized in the endomyseum, in close vicinity of the basal lamina (arrows), resulting in less staining in the middle of the endomysium. In contrast, collagen fibrils were more diffusely localized throughout the endomysium in Col12a1$^{-/-}$ (**F**). Bars = 200 nm.

spine in these animals had revealed kyphoscoliosis as well as a doubling of the spinous process (24). This was not seen on spine X rays of the three human patients (data not shown).

Skeletal muscles from 9-month-old *Col12a1*$^{-/-}$ animals and their litter mate controls were dissected and weighed. When corrected for overall body weight [which as opposed to the weight difference at P30 (24), at the age of 9 months it was no longer significantly different between *Col12a1*$^{-/-}$ and wild-type animals], muscle weights were not statistically different in the collagen XII-deficient animals compared with their littermate controls; however, when taken at their absolute values, the weights for tibialis anterior (TA), gastrocnemius, quadriceps and extensor digitorum longus (EDL) muscles were significantly lower in the *Col12a1*$^{-/-}$ animals (Fig. 6A). Muscles were then sectioned at mid-belly for histological analysis. H&E-stained sections from TA, soleus, gastrocnemius and quadriceps were examined for nuclear position and for evidence for degeneration and regeneration. There were no degenerating fibers and no clearly regenerating fibers; however, there was a very mild increase in central nucleation in the quadriceps muscle (1.75 versus 0.91%, $P < 0.05$), while this was not found in the other hindlimb muscles examined (data not shown). Fiber size distribution was assessed using histograms generated using the minimal Feret's diameter method (25). There was no statistically significant difference in fiber diameter distribution between wild-type and *Col12a1*$^{-/-}$ animals (Fig. 6D–F). We next proceeded to determine the

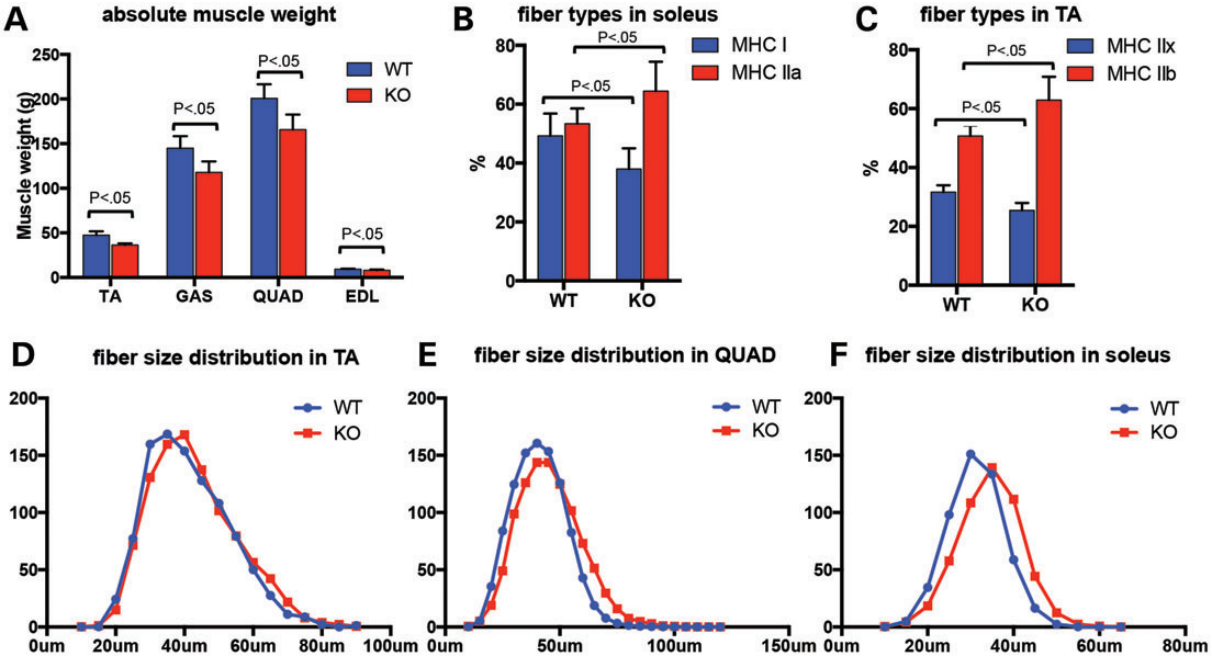

Figure 6. Absolute muscle weight, fiber-type composition and fiber size distribution in *Col12a1*$^{-/-}$ mice: (**A**) in *Col12a1*$^{-/-}$ mice, there were significant decreases ($P < 0.05$) in absolute muscle weight of the TA (36.4 ± 1.8 versus 47.3 ± 4.4 mg), gastrocnemius (GAS) (117.9 ± 12.2 versus 144.9 ± 13.5 mg), quadriceps (QUAD) (165.7 ± 16.9 versus 200.7 ± 15.7 mg) and EDL (8.07 ± 0.7 versus 9.2 ± 0.8 mg); (**B**) in the soleus, there was an increase in fast fiber type IIa (64.4 versus 53.4%, $P < 0.05$) and a decrease in slow fiber type I (38 versus 49.2%, $P < 0.05$) compared with litter mate controls, (**C**) similarly in the TA muscle there was an increase in type IIb (62.9 versus 50.7%, $P < 0.05$) and decrease in type IIx (25.4 versus 31.6%, $P < 0.05$) compared with litter mate controls; (**D**) no significant difference in fiber size distribution (minimal Feret's diameter) was found between wild-type and *Col12A1*$^{-/-}$ mice, as shown for the TA, QUAD and soleus muscles.

distribution of fiber types in various muscles of the hindlimb by immunhistochemical determination of fiber types using antibodies against specific MHC types. In the soleus, there was an increase in fast fiber type IIa and a decrease in slow fiber type I compared with litter mate controls [64.4 versus 53.4% type IIa fibers ($P < 0.05$), 38 versus 49.2% type I fibers ($P < 0.05$), Fig. 6B]; the expected distribution before fiber types normally shift to a more slow, i.e. a type I predominant phenotype that is typical for the adult soleus muscle (26,27). Similarly, an increase of type IIb (62.9 versus 50.7%, $P < 0.05$) and decrease of type IIx (25.4 versus 31.6%, $P < 0.05$) were observed in Col12a1$^{-/-}$ TA muscle (Fig. 6C).

Transmission electron microscopic analysis on *Col12a1*$^{-/-}$ muscle compared with wild-type muscle revealed a difference in the distribution of large collagen fibrils in the endomysium: whereas in the wild-type muscle, the fibrils were located in close proximity to the basement membrane of the fibers, in *Col12a1*$^{-/-}$ muscle the distribution was changed in that the fibrils were more located in the middle of the endomysium, which was clearly seen at P30 (Fig. 5E and F), but was also notable at P3 and P14 (Supplementary Material, Fig. S1A). There was also an apparent difference in the contour of the sarcolemma of individual muscle fibers which had a more wavy appearance in the *Col12a1*$^{-/-}$ compared with wild-type at days P3 and P30, although we did not appreciate a difference in the density or continuity of the basement membrane around the muscle fibers (Supplementary Material, Fig. S1B).

Physiological measurements were undertaken on isolated EDL muscles from *Col12a1*$^{-/-}$ animals compared with wild-type littermate controls. Even though the muscles were smaller in mass, there was no statistical difference in calculated cross-sectional area (Fig. 7A). However, isometric tetanic force production was depressed by 18% (Fig. 7B), leading to significantly lower specific force (force normalized to cross-sectional area) (Fig. 7C). Surprisingly, compared with muscle from wild-type animals, there was less force drop on the eccentric contraction paradigm in the muscle from the collagen XII-deficient animals (Fig. 7E). In contrast, there was significant decrease in passive force generation, i.e. the force generated by the muscle when passively stretched was less in collagen XII-deficient muscle (Fig. 7D).

DISCUSSION

Collagen XII is a member of the FACIT family of collagens. While its location in collagen type I containing connective tissue structures such as skin, tendons and ligaments, cartilage, blood vessels, epimysium, perimysium and cornea and its interactions with tenascin-X has been known (13,28,29), the clinical consequences of mutations in human or mouse affecting collagen XII have been difficult to predict. We now report on the first human mutations in COL12A1 and correlate the human clinical phenotype to the neuromuscular phenotype in a mouse model in which *Col12a1* had been inactivated by homologous recombination. Although so far we have only ascertained three patients in two families, we can already conclude that mutations in COL12A1 are associated with a spectrum of severity and can be caused by both recessive and dominant genetic mechanisms. We discuss the main findings below.

Patients A1 and A2 represent a severe phenotype with complete absence of collagen XII as a result of a homozygous loss

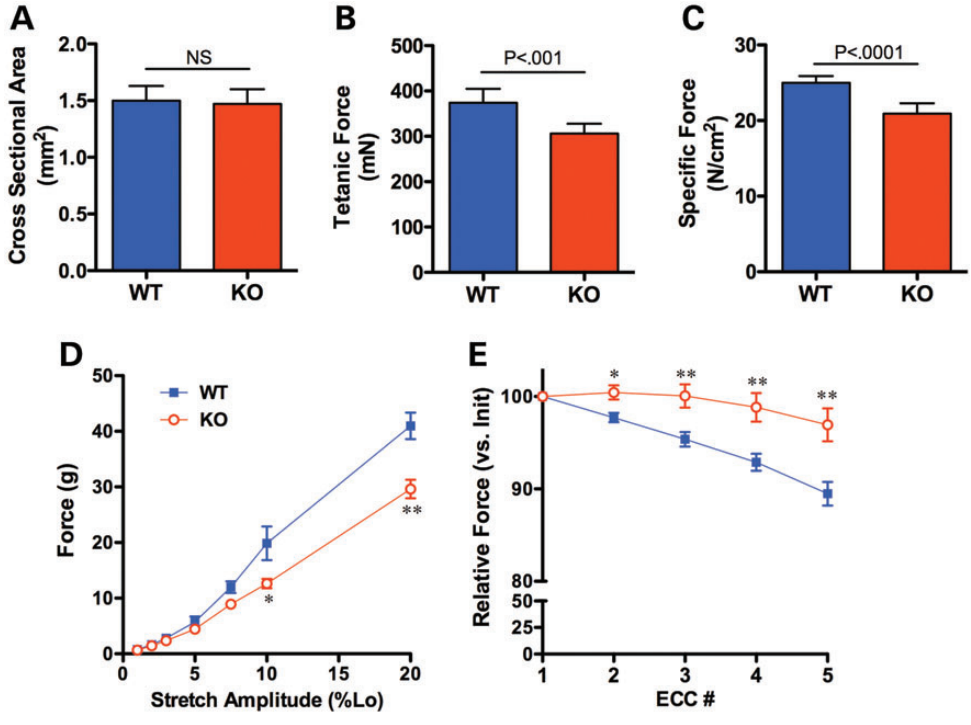

Figure 7. Functional assessment of isolated EDL muscles from *Col12a1*$^{-/-}$ mice. There was no difference in muscle size between muscles from wild-type and *Col12a1*$^{-/-}$ mice (**A**). However, isometric tetanic force was significantly lower in the muscles from *Col12a1*$^{-/-}$ mice (**B**), resulting in a 16% decrement in specific force (**C**). Passive tension was greater in muscles from WT mice than from *Col12a1*$^{-/-}$ mice, particularly at higher amplitudes of stretch (**D**). The muscles from *Col12a1*$^{-/-}$ mice were protected from the loss of force production that occurs during eccentric contractions (**E**). Data represent mean ± SEM for $n = 7$ muscles per genotype. $^{*}P < 0.05$, $^{**}P < 0.01$ for unpaired *t*-tests.

of function mutation, resulting in a syndrome with prominent joint hypermobility, milder proximal contractures as well as muscle weakness precluding ambulation, while patient B has a milder phenotype on the basis of a dominantly acting *de novo* missense mutation. Even though these features are reminiscent of the collagen VI-related Ullrich congenital muscular dystrophy (1,4), there are also clinical differences in that the joint hypermobility was even more pronounced and widespread compared with a typical infant with Ullrich, which is often associated with more significant proximal contractures. Also, the long face and high palate would be somewhat unusual for a typical Ullrich patient. Early kyphosis followed by scoliosis can occur in both as well as in the kyphoscoliotic type of EDS, which can also include significant neuromuscular weakness (30). However, the respiratory insufficiency in patient A1 was even earlier than expected in typical Ullrich (31,32), pointing to significant weakness of the respiratory muscles.

Patient B1 has a milder phenotype allowing for the achievement of ambulation. His joint hypermobility, weakness, abnormal findings on muscle ultrasound (increased granular echogenicity suggesting the presence of smaller fibers and/or of increased connective tissue) and mildly abnormal biopsy again suggest involvement of both tendons as well as of muscle. His muscle strength appeared to improve, arguing against a degenerative course of the muscle component. There was kyphosis but not yet scoliosis.

The mechanism of disease in family A is complete loss of function of collagen XII on the basis of the homozygous splice site mutation c.8006+1G>A. The resulting exclusion of exon 50 from the COL12A1 transcript results in a frame shift with a predicted termination codon occurring before the collagenous domain. Thus, the resulting protein would be assembly-incompetent and likely is rapidly degraded as we did not detect any immunoreactivity for collagen XII neither in the matrix nor within the cells using collagen type XII-specific antibody KR75. This mutation trigger nonsense-mediated mRNA decay, as shown by relative quantitative RT-PCR that COL12A1 transcription level in patient A1 fibroblast is only 3% of that in normal control fibroblasts (average of eight different normal control cell lines) (Fig. 3L). If there is any truncated protein being translated, it would be assembly-incompetent and likely is rapidly degraded as we did not detect any immunoreactivity for collagen XII neither in the matrix nor within the cells using collagen type XII-specific antibody KR75. We assume that haploinsufficiency for collagen type XII as seen in the two carrier parents is associated with a mild phenotype as both parents had delayed motor development but reached normal strength in adulthood. That haploinsufficiency may be associated with some clinical consequences is also suggested by a contiguous gene micro-deletion syndrome that involves COL12A1 among additional genes within in the deletion and in which the patients were also reported to exhibit marked joint hyperlaxity (among other clinical features) (33).

The *de novo* mutation found in patient B1 on the other hand acts in a dominant way. This missense mutation p. Ile2334Thr is directly adjacent to and interferes with a MIDAS domain in collagen XII. Molecular modeling predicts that the octahedral coordination sphere of the metal binding site of the MIDAS domain will be disrupted by this substitution, likely diminishing its interactive

capability that is thought to be important in protein/protein interactions. We assume that the mutation exerts a dominant negative effect on the collagen XII homotrimer as the boy's phenotype is clearly more severe compared with the much milder features seen in the haploinsufficient parents of family A. If the mutant chain is assumed to be incorporated into the trimer efficiently, only 25% of resulting trimeric collagen XII molecules would be wild-type, possibly interfering with secretion and/or with formation and interactions in the matrix. Our immunocytochemical analysis of the fibroblasts showed a significantly reduced collagen XII extracellular matrix formation in 4-day post-confluent culture. Immunoblotting analysis showed the soluble collagen XII in the patient fibroblast conditioned medium was increased, while the collagen XII from the cell layer kept the same level as in normal control fibroblasts. Relative quantitative RT-PCR results showed that there was no up-regulation of COL12A1 transcription in patient B fibroblast comparing with normal control fibroblasts (average of eight different normal control cell lines) (Fig. 3L). These data suggest that the mutant collagen XII is in fact capable of being secreted, but that this secreted collagen XII is then not able to assemble into a stable (and therefore immuno-stainable) extracellular collagen XII matrix, perhaps remaining in the soluble fraction accounting for the increased signal on western blot. Additional evidence for the existence of a dominant mechanism for collagen XII mutations is provided in the paper by Hicks *et al*. (34). describing dominant mutation in COL6A1 in patients with a Bethlem myopathy like phenotype.

In the tenascin-X-deficient mouse, a 70% deficiency of collagen XII in muscle and skin has been observed consistent with an established interaction between collagen XII and tenascin-X (13) (Supplementary Material, Fig. S2), while deficiency of tenascin-X has been associated with decreased collagen VI in fibroblasts (35) although not in human muscle tissue deficient in tenascin X (36). It is of this note that there was no obvious deficiency of either collagen VI or tenascin-X immunoreactivity apparent in the collagen XII negative muscle biopsy (data not shown). We had the opportunity to stain muscle biopsy slides from two previously reported patients with tenascin-X deficient EDS (37,38) but did not find a deficiency of collagen XII immunoreactivity (Supplementary Material, Fig. S3). It is possible that this is due to differences between mouse and human as far as tissue and temporal expression of collagen XII is concerned (16).

A mouse model of collagen XII inactivation generated by targeted inactivation of the gene at P30 showed abnormalities in the formation of vertebral bodies (duplication of the spinous vertebral processes) as well as a short and thin femurs (39) as well as abnormalities of bone matrix formation and orientation of osteoblasts, while their neuromuscular phenotype had not been analyzed. These potential orthopedic aspects of the phenotype were not obvious in the patients of family A, who had X-ray examinations of the spine and long bones as part of their orthopedic evaluation. Such a difference in degree of weakness is also known from the collagen VI-deficient mouse model (40), which also shows much milder weakness compared with the human patients with a complete deficiency of collagen VI (1). One reason could be subtle differences in tissue expression of collagen XII, which in human muscle maintains a presence in the endomysium, while in the mouse endomysial localization is seen during development, but no longer in the adult mouse (16). Similar to the scoliosis and kyphosis seen in the human patients, the collagen XII-deficient mouse also had kyphoscoliosis. The differences could also be an effect of the genetic background in the mice on which the mutation occurred (41). In the case of complete collagen XII deficiency, the mutation is on a mixed genetic background as we have not yet been able to backcross the mice onto a pure genetic background, as there was neonatal lethality due to unknown reason. Thus, even though the *Col12a1*$^{-/-}$ mouse models some aspects of the human disease such as the connective tissue aspect, it also shows differences in the degree of muscle weakness, with the human null situation causing a much more significant disease.

In vitro physiological analysis revealed a deficiency in absolute and specific force [although EDL muscles from knockout mice tended to be shorter, but there was no significant difference in CSA (Fig. 7A)]. In addition, this analysis did confirm an abnormality of the muscle tendon unit, but it is significant that the findings obtained are markedly different from those in a primary muscle disorder such as dystrophin deficiency in the mdx mouse. In the mdx model of dystrophin deficiency, there is a conspicuous force drop with repetitive contractions following successive lengthening (eccentric contraction) compared with normal muscle (42–44). In this contraction paradigm the sarcomere is progressively lengthened in between contractions beyond its optimal length to force ratio. In contrast, in the *Col12a1*$^{-/-}$ animals, the isolated muscle in this paradigm is protected from the force drop that occurs with the successive lengthening, suggesting that the lengthening of the muscle is not completely transmitted to the sarcomere as the contractile protecting it from the damage arising from the lengthening. At the same time, we found a deficiency in passive force generation, i.e. the stretched muscle in collagen XII-deficient animals generates less force as a passive unit compared with normal muscle. Both the relative protection from eccentric force drop as well as the decreased passive force likely are a reflection of an increased elasticity (and hence compliance) of the muscle tissue, suggesting a more pliant matrix with decreased ability to transmit force within the entire matrix-muscle unit. This would directly affect force transmission in the intact muscle-tendon-bone unit (as suggested by the decreased grip strength). This deficit in force transmission is likely to affect both longitudinal as well as lateral force transmission, given the distribution of collagen XII in and around muscle. That there are changes in the matrix composition which may play a role in this effect is also supported by our observation on transmission electron micrographs of an altered distribution of endomysial large collagen fibrils in *Col12A1*$^{-/-}$ muscle (Fig. 5E and F). The functional consequences may be similar to findings in *Tnxb* knockout mice and TNX-deficient EDS patients who also display an increased compliance of matrix-muscle unit (45,46). Together, these models show the mechanism of muscle weakness if not the molecular motor but the muscle matrix is deficient.

Although absolute muscle weights tended to be lower in *Col12a1*$^{-/-}$ animals (Fig. 6A), we did not find formal evidence for muscle fiber atrophy on measuring fiber size distributions (Fig. 6D). However, in the soleus, we did observe a higher proportion of type II fibers when compared with littermate controls. The fiber composition in the soleus in these 9-month-old knock-out animals resembled the fiber-type composition observer in younger (1 months old) wild-type animals (26). The soleus muscle in adult animals is a predominantly slow, i.e. fiber type I-dominated muscle that is involved maintaining position rather

than in burst activity. Between 1and 8 months postnatal development, there is a shift from a predominantly fast glycolytic (>60% type II) soleus muscle that is still present at 3 months to the more slow, oxidative fiber type I predominant muscle (60% type I) of the adult animal (26). This transition of fiber types likely is dependent on normal activity as well as normal constant load. This transition has been shown to be abnormal in other early onset muscle disease in the mouse, in particular in the dy2J model of LAMA2-related (merosin-deficient) congenital muscular dystrophy (26). Unloading of the hindlimb in the normal adult animal has also been shown to change the fiber-type composition of the soleus muscle in favor of type IIa fibers (47,48). It is thus possible that the change in matrix elasticity with resulting diminished passive force transmission and diminished mechanical load in the *Col12A1*$^{-/-}$ mice also plays a role in delay in fiber-type switching that we had observed in the soleus muscle. There are previous data to suggest that a mechanical stimulus has to be transmitted to the muscle fibers for the successful fiber-type switching to occur. Mechanical unloading of muscle is a potent trigger for changes in fiber-type composition (47–49) of the muscle as well as for the engagement of muscle atrophy pathways. We thus postulate that the changes in matrix physical properties to some extent represent a functional mechanical unloading of the muscle.

Our observation of a novel overlap disorder affecting connective tissue and muscle adds to the growing evidence from mouse models and human disease supporting an important role for the extracellular matrix for the maintenance and function of muscle (50). Functions for which the extracellular matrix of muscle (the 'myomatrix') has been implicated include patterning, force transmission, scaffold for regeneration, stem cell/muscle precursor niche, determinant for differentiation, reservoir and regulator of signaling, pathway for inflammatory cells and others. Here, we implicate the changes in mechanical matrix properties as mediating important aspects of the phenotype of collagen XII deficiency, while it is still possible that other consequences of an altered extracellular matrix may also participate in the pathogenesis of the muscle weakness that is seen in this condition.

MATERIALS AND METHODS

Haplotype analysis and sequencing

A whole genome screen was performed on all five individuals from family A using the Illumina Linkage Panel IV Array (San Diego, CA, USA), which includes 5861 informative SNP markers distributed evenly across the human genome with an average distance of 0.64 cM. DNA was extracted from EDTA-treated blood with Puregene Genomic DNA Purification Kit from Gentra Systems (Minneapolis, MN, USA), genotyping was done at NAPCore of Children's Hospital of Philadelphia according to Illumina's protocol. Haplotype analysis was done with linkage analysis software Merlin (51). For mutation analysis, total RNA was extracted from dermal fibroblast cultures and reverse transcribed to cDNA. Primers were designed to amplify the entire coding region of COL12A1 in 12 fragments. Fragments were run on a gel for size determination and sequenced. Mutations were confirmed on genomic DNA extracted from the dermal fibroblasts and from whole blood by designing primers specific for the exon in questions followed by direct sequencing. Primer sequences are listed in Supplementary Material, Table S1.

Mutation modeling

The homology modeling approach was used to generate 3D structures (wild-type and mutant versions) of the human collagen XII VWA domain composed of 143 amino acids (16.3 kDa). The crystal structure coordinates of the VWA domain of alpha2beta1 integrin (52) were used as one of the templates showing about 45% sequence identity and about 63% sequence similarity. The Deep View Tool of the Swiss Model web based server (23) was used to align sequences of different known VWA structures, then the human collagen XII sequence was threaded to the crystal structure of the alpha2beta1 VWA domain and approached for model building using Modeller (53). After building the 3D model of the collagen XII VWA domain, all atomic positions are locked and required hydrogen atoms were added. The Protein Structure & Model Assessment Tools (54) was used to verify the quality of both VWA models. For subsequent calculations including molecular dynamic simulation and characterizations of point mutations, we performed conjugated gradient minimizations in CNS (55) in combination with molecular mechanics (MM2) and then performed molecular dynamics simulation at 1000 k for 50 ps for further optimization [GROMACS (56)].

Human fibroblast culture and muscle biopsy analysis

Dermal fibroblasts were grown in Dulbecco's modified Eagle medium with 10% fetal bovine serum (Life Technologies) in 5% CO_2 at 37°C. For immunofluorescence staining and immunoblotting, cells were cultured in the presence of 50 μg/ml L-ascorbic acid phosphate (Wako) until 4 days post-confluent as described (5). Frozen muscle biopsies were obtained from the previous workup and 9 μm cross-sections were used for immunofluorescence staining. For immunofluorescence staining, 4% paraformaldehyde fixed fibroblast cultures or cold methanol fixed muscle sections were incubated with primary antibodies at 4°C overnight [anti-collagen XII (KR75, KG76—both these antibodies recognize the fibronectin III repeats 14 to 18) (23,57), anti-collagen VI (MAB1944, Millipore, Billerica, MA, USA) and anti-laminin γ1 (L9393, Sigma Aldrich, MO, USA)], the antibody labeling was detected with secondary antibodies for 1 h at room temperature (Alexa 488-conjugated goat anti-rabbit IgG, Alex 568-conjugated goat anti-mouse IgG or Alex 568-conjugated goat anti-guinea pig IgG (Molecular Probes, Eugene, OR, USA)] and then prepared for imaging. Immunoblotting analysis of culture medium and cell layers from confluent fibroblasts were performed using antibody specific for collagen XII KR75, antibody specific for α2 (VI) collagen chain (58), antibody specific for fibronectin (F3648, Sigma Aldrich) and tubulin antibody (T5168, Sigma Aldrich). To compare COL12A1 transcription level in fibroblast cells from patients and normal controls, total RNA was isolated from confluent fibroblasts cultures using RNeasy mini Kit (Qiagen, USA). cDNA was reverse transcribed with SuperScript® III Reverse Transcriptase (Life Technologies). Relative quantitative PCR was performed on an ABI PRISM® 7900HT Sequence Detection System with Universal Probe Library assay (UPL) (Roche Applied Science, IN, USA) (Supplementary Material, Table S1). Relative quantification

analysis of COL12A1 transcription was done using the comparative C_T method (59).

Mouse muscle histological analysis

We used *Col12a1*$^{-/-}$ mice generated by targeted deletion of exons 2–5 as described in detail previously (24). Individual mouse muscles [TA, gastrocnemius muscle (Gas), quadriceps femoris muscle (Quad), EDL muscle and soleus muscle] were isolated from eight *Col12a1*$^{-/-}$ mice and eight littermate wild-type control mice at 9 months of age. Isolated muscles were snap frozen in isopentane cooled in liquid nitrogen and cross-sections of 9 μm were cut at mid-belly of the muscles. For the muscle fiber-type study, muscle sections were incubated with myosin heavy chain-specific antibodies (A4.840, A4.74, BF-35 and BF-F3, DSHB, University of Iowa) over night at 4°C, the antibody labeling was detected with Alexa 488 conjugated goat anti-mouse IgG (Molecular Probes) for 1 h at room temperature and then prepared for imaging. For muscle morphological studies, muscle fiber size was determined by using minimal Feret's diameter of a fiber cross-section (25). In brief, muscle fiber boundaries were demarcated using staining with Alexa 488 conjugated wheat germ agglutinin (Molecular Probes), images of entire muscle cross-sections were captured with Nikon Eclipse Ti microscope with mobilized stage. Muscle fiber outline was identified and minimal Feret's diameter was measured with automatic analysis software NIS Element (Nikon Instrument Inc, NY, USA).

Transmission electron microscopy

Gastrocnemius muscles from *Col12A1*$^{-/-}$ and wild-type mice between P3 and P30 were analyzed by transmission electron microscopy. Briefly, muscles were dissected and fixed in 4% paraformaldehyde, 2.5% glutaraldehyde, 0.1 M sodium cacodylate, pH 7.4, with 8.0 mM $CaCl_2$ at 4°C for 2 h (60). This was followed by post-fixation with 1% osmium tetroxide, dehydration in an ethanol series, followed by propylene oxide and the tissue samples were infiltrated and embedded in a mixture of EMbed 812, nadic methyl anhydride, dodecenylsuccinic anhydride and DMP-30 (Electron Microscopy Sciences, Hatfield, PA, USA). Thin sections were post-stained with 2% aqueous uranyl acetate and 1% phosphotungstic acid, pH 3.2. Cross-sections were examined at 80 kV using JEOL 1400 transmission electron microscope equipped with a Gatan Ultrascan US1000 2K digital camera.

Grip strength assessment

To assess musculoskeletal/motor function impairment of the *Col12a1* mice, grip strength was evaluated at P30 using both the hanging as well as a grip strength meter (San Diego Instrument). The latter was used to record the peak force the animal exerts in grasping a grip placed at their fore limb. The grip strength meter was positioned horizontally and the mouse was held by the tail and lowered toward the grip strength platform. The animal was allowed to grasp the fore limb grip with its forepaws and was then pulled steadily by the tail away from the rod until the mouse's grip was broken. The force applied to the grip just before the animal loses its grip is recorded as the peak tension. Ten measurements for each mouse were recorded and the average force was used to represent the grip strength for individual mouse. For the hanging test, mice were placed on a stick and left hanging, recording the time until they fell off. We measured the hanging time. Five measurements for each mouse were recorded and the average time was normalized to body weight since the body weight is a variable in this method (heavier body weight promotes earlier fall off at similar grip strength). The data were expressed as average minutes/body weight. Wild-type mice are able to stay on the stick for a long time, so the time left hanging was limited to 5 min. No mutant mice exceeded this time in pilot experiments.

Mouse muscle physiology

Physiological analysis was performed on isolated EDL muscles, isolated from 9-month-old male *Col12a1*$^{-/-}$ mice and littermate control mice (24), which were dissected after the animals had been sacrificed. Whole muscle mechanics were performed with a commercially available physiology apparatus with associated software (Aurora Scientific, Ontario, Canada) as previously described (61–63). Briefly, mice were anesthetized with ketamine/xylazine. Muscles were removed and placed in a bath of Ringers solution gas-equilibrated with 95% O_2–5% CO_2. Sutures were attached to the distal and proximal muscle tendon junctions of the EDL. Optimum length (L_o) of each muscle was defined as the length at which maximal twitch force developed from supramaximal stimulation (@120 Hz, 40 V). For active force production, each muscle was subjected to three 500 ms tetanic contractions at L_o with 5 min between each trial. A series of five eccentric contractions was delivered to the muscle. Each contraction, separated by a period of 5 min, consisted of an 80-Hz, 700-ms pulse delivered via two parallel platinum plate electrodes, where a stretch of 10% L_o was imposed on the muscle in the last 200 ms of the contraction. For passive tension measurements, EDL muscles were subjected to sinusoidal length change cycles at a frequency of 1 Hz from 1 to 20% of L_o. The maximum force achieved during five cycles was recorded for each amplitude. Eight *Col12a1*$^{-/-}$ animals from three litters and eight littermate controls were examined.

SUPPLEMENTARY MATERIAL

Supplementary Material is available at *HMG* online.

ACKNOWLEDGEMENTS

We would like to thank the families for their participation and support of this research.

Conflict of Interest statement. None declared.

FUNDING

Work in C.G.B.'s lab is supported by NINDS/NIH intramural research funds. The work was started with support of a grant of the MDA-USA to C.G.B. Supported by the Deutsche Forschungsgemeinschaft SFB 829 grant A2 (M.K.) and by the Köln Fortune Programme of the Medical Faculty (M.K.). Work in in E.R.B.'s lab was supported by a Paul Wellstone Muscular

Dystrophy Cooperative Research Center (U54 AR052646). J.S. was supported by the Heart and Stroke Foundation Canada and the Canada Research Chair Program. D.B. was supported by NIAMS/NIH AR044745.

REFERENCES

1. Bonnemann, C.G. (2011) The collagen VI-related myopathies: muscle meets its matrix. *Nat. Rev. Neurol.*, **7**, 379–390.
2. Kirschner, J., Hausser, I., Zou, Y., Schreiber, G., Christen, H.J., Brown, S.C., Anton-Lamprecht, I., Muntoni, F., Hanefeld, F. and Bonnemann, C.G. (2005) Ullrich congenital muscular dystrophy: connective tissue abnormalities in the skin support overlap with Ehlers-Danlos syndromes. *Am. J. Med. Genet. A*, **132**, 296–301.
3. Schessl, J., Goemans, N.M., Magold, A.I., Zou, Y., Hu, Y., Kirschner, J., Sciot, R. and Bonnemann, C.G. (2008) Predominant fiber atrophy and fiber type disproportion in early Ullrich disease. *Muscle Nerve*, **38**, 1184–1191.
4. Allamand, V., Briñas, L., Richard, P., Stojkovic, T., Quijano-Roy, S. and Bonne, G. (2011) ColVI myopathies: where do we stand, where do we go? *Skelet. Muscle*, **1**, 30.
5. Zou, Y., Zhang, R.Z., Sabatelli, P., Chu, M.L. and Bonnemann, C.G. (2008) Muscle interstitial fibroblasts are the main source of collagen VI synthesis in skeletal muscle: implications for congenital muscular dystrophy types Ullrich and Bethlem. *J. Neuropathol. Exp. Neurol.*, **67**, 144–154.
6. Braghetta, P., Ferrari, A., Fabbro, C., Bizzotto, D., Volpin, D., Bonaldo, P. and Bressan, G.M. (2008) An enhancer required for transcription of the Col6a1 gene in muscle connective tissue is induced by signals released from muscle cells. *Exp. Cell Res.*, **314**, 3508–3518.
7. Zhang, G., Young, B.B. and Birk, D.E. (2003) Differential expression of type XII collagen in developing chicken metatarsal tendons. *J. Anat.*, **202**, 411–420.
8. Nishiyama, T., McDonough, A.M., Bruns, R.R. and Burgeson, R.E. (1994) Type XII and XIV collagens mediate interactions between banded collagen fibers in vitro and may modulate extracellular matrix deformability. *J. Biol. Chem.*, **269**, 28193–28199.
9. Jin, X., Iwasa, S., Okada, K., Ooi, A., Mitsui, K. and Mitsumata, M. (2003) Shear stress-induced collagen XII expression is associated with atherogenesis. *Biochem. Biophys. Res. Commun.*, **308**, 152–158.
10. Arai, K., Nagashima, Y., Takemoto, T. and Nishiyama, T. (2008) Mechanical strain increases expression of type XII collagen in murine osteoblastic MC3T3-E1 cells. *Cell Struct. Funct.*, **33**, 203–210.
11. Font, B., Eichenberger, D., Rosenberg, L.M. and van der Rest, M. (1996) Characterization of the interactions of type XII collagen with two small proteoglycans from fetal bovine tendon, decorin and fibromodulin. *Matrix Biol.*, **15**, 341–348.
12. Font, B., Eichenberger, D., Goldschmidt, D., Boutillon, M.M. and Hulmes, D.J. (1998) Structural requirements for fibromodulin binding to collagen and the control of type I collagen fibrillogenesis—critical roles for disulphide bonding and the C-terminal region. *Eur. J. Biochem.*, **254**, 580–587.
13. Veit, G., Hansen, U., Keene, D.R., Bruckner, P., Chiquet-Ehrismann, R., Chiquet, M. and Koch, M. (2006) Collagen XII interacts with avian tenascin-X through its NC3 domain. *J. Biol. Chem.*, **281**, 27461–27470.
14. Koch, M., Bohrmann, B., Matthison, M., Hagios, C., Trueb, B. and Chiquet, M. (1995) Large and small splice variants of collagen XII: differential expression and ligand binding. *J. Cell Biol.*, **130**, 1005–1014.
15. Wälchli, C., Koch, M., Chiquet, M., Odermatt, B.F. and Trueb, B. (1994) Tissue-specific expression of the fibril-associated collagens XII and XIV. *J. Cell. Sci.*, **107**(Pt 2), 669–681.
16. Oh, S.P., Griffith, C.M., Hay, E.D. and Olsen, B.R. (1993) Tissue-specific expression of type XII collagen during mouse embryonic development. *Dev. Dyn.*, **196**, 37–46.
17. Böhme, K., Li, Y., Oh, P.S. and Olsen, B.R. (1995) Primary structure of the long and short splice variants of mouse collagen XII and their tissue-specific expression during embryonic development. *Dev. Dyn.*, **204**, 432–445.
18. Pan, T.C., Zhang, R.Z., Markova, D., Arita, M., Zhang, Y., Bogdanovich, S., Khurana, T.S., Bonnemann, C.G., Birk, D.E. and Chu, M.L. (2013) Col6a3 deficiency in mice leads to muscle and tendon defects similar to human collagen VI congenital muscular dystrophy. *J. Biol. Chem.*, **288**, 14320–14331.
19. Bader, H.L., Keene, D.R., Charvet, B., Veit, G., Driever, W., Koch, M. and Ruggiero, F. (2009) Zebrafish collagen XII is present in embryonic connective tissue sheaths (fascia) and basement membranes. *Matrix Biol.*, **28**, 32–43.
20. Tozer, E.C., Liddington, R.C., Sutcliffe, M.J., Smeeton, A.H. and Loftus, J.C. (1996) Ligand binding to integrin alphaIIbbeta3 is dependent on a MIDAS-like domain in the beta3 subunit. *J. Biol. Chem.*, **271**, 21978–21984.
21. San Sebastian, E., Mercero, J.M., Stote, R.H., Dejaegere, A., Cossío, F.P. and Lopez, X. (2006) On the affinity regulation of the metal-ion-dependent adhesion sites in integrins. *J. Am. Chem. Soc.*, **128**, 3554–3563.
22. Leitinger, B., McDowall, A., Stanley, P. and Hogg, N. (2000) The regulation of integrin function by Ca(2+). *Biochim. Biophys. Acta*, **1498**, 91–98.
23. Agarwal, P., Zwolanek, D., Keene, D.R., Schulz, J.N., Blumbach, K., Heinegård, D., Zaucke, F., Paulsson, M., Krieg, T., Koch, M. and Eckes, B. (2012) Collagen XII and XIV, new partners of cartilage oligomeric matrix protein in the skin extracellular matrix suprastructure. *J. Biol. Chem.*, **287**, 22549–22559.
24. Izu, Y., Sun, M., Zwolanek, D., Veit, G., Williams, V., Cha, B., Jepsen, K.J., Koch, M. and Birk, D.E. (2011) Type XII collagen regulates osteoblast polarity and communication during bone formation. *J. Cell Biol.*, **193**, 1115–1130.
25. Briguet, A., Courdier-Fruh, I., Foster, M., Meier, T. and Magyar, J.P. (2004) Histological parameters for the quantitative assessment of muscular dystrophy in the mdx-mouse. *Neuromuscul. Disord.*, **14**, 675–682.
26. Ovalle, W.K., Bressler, B.H., Jasch, L.G. and Slonecker, C.E. (1983) Abnormal distribution of fiber types in the slow-twitch soleus muscle of the C57BL/6J dy2J/dy2J dystrophic mouse during postnatal development. *Am. J. Anat.*, **168**, 291–304.
27. Wigston, D.J. and English, A.W. (1992) Fiber-type proportions in mammalian soleus muscle during postnatal development. *J. Neurobiol.*, **23**, 61–70.
28. Sugrue, S.P., Gordon, M.K., Seyer, J., Dublet, B., van der Rest, M. and Olsen, B.R. (1989) Immunoidentification of type XII collagen in embryonic tissues. *J. Cell Biol.*, **109**, 939–945.
29. Thierry, L., Geiser, A.S., Hansen, A., Tesche, F., Herken, R. and Miosge, N. (2004) Collagen types XII and XIV are present in basement membrane zones during human embryonic development. *J. Mol. Histol.*, **35**, 803–810.
30. Voermans, N.C., Bonnemann, C.G., Lammens, M., van Engelen, B.G. and Hamel, B.C. (2009) Myopathy and polyneuropathy in an adolescent with the kyphoscoliotic type of Ehlers-Danlos syndrome. *Am. J. Med. Genet. A*, **149A**, 2311–2316.
31. Nadeau, A., Kinali, M., Main, M., Jimenez-Mallebrera, C., Aloysius, A., Clement, E., North, B., Manzur, A.Y., Robb, S.A., Mercuri, E. and Muntoni, F. (2009) Natural history of Ullrich congenital muscular dystrophy. *Neurology.*, **73**, 25–31.
32. Yonekawa, T., Komaki, H., Okada, M., Hayashi, Y.K., Nonaka, I., Sugai, K., Sasaki, M. and Nishino, I. (2013) Rapidly progressive scoliosis and respiratory deterioration in Ullrich congenital muscular dystrophy. *J. Neurol. Neurosurg. Psychiatry*, **84**, 982–988.
33. Van Esch, H., Rosser, E.M., Janssens, S., Van Ingelghem, I., Loeys, B. and Menten, B. (2010) Developmental delay and connective tissue disorder in four patients sharing a common microdeletion at 6q13–14. *J. Med. Genet.*, **47**, 717–720.
34. Hicks, D., Farsani, G.T. and Laval, S. Mutations in the Collagen XII gene define a new form of extracellular matrix related myopathy. *Hum. Mol. Genet.* doi:10.1093/hmg/ddt637.
35. Minamitani, T., Ariga, H. and Matsumoto, K. (2004) Deficiency of tenascin-X causes a decrease in the level of expression of type VI collagen. *Exp. Cell Res.*, **297**, 49–60.
36. Pénisson-Besnier, I., Allamand, V., Beurrier, P., Martin, L., Schalkwijk, J., van Vlijmen-Willems, I., Gartioux, C., Malfait, F., Syx, D., Macchi, L. *et al.* (2013) Compound heterozygous mutations of the TNXB gene cause primary myopathy. *Neuromuscul. Disord.*, **23**, 664–669.
37. Schalkwijk, J., Zweers, M.C., Steijlen, P.M., Dean, W.B., Taylor, G., van Vlijmen, I.M., van Haren, B., Miller, W.L. and Bristow, J. (2001) A recessive form of the Ehlers-Danlos syndrome caused by tenascin-X deficiency. *N. Engl. J. Med.*, **345**, 1167–1175.
38. Voermans, N.C., Jenniskens, G.J., Hamel, B.C., Schalkwijk, J., Guicheney, P. and van Engelen, B.G. (2007) Ehlers-Danlos syndrome due to tenascin-X deficiency: muscle weakness and contractures support overlap with collagen VI myopathies. *Am. J. Med. Genet. A*, **143A**, 2215–2219.
39. Izu, Y., Ansorge, H.L., Zhang, G., Soslowsky, L.J., Bonaldo, P., Chu, M.L. and Birk, D.E. (2011) Dysfunctional tendon collagen fibrillogenesis in collagen VI null mice. *Matrix Biol.*, **30**, 53–61.

40. Bonaldo, P., Braghetta, P., Zanetti, M., Piccolo, S., Volpin, D. and Bressan, G.M. (1998) Collagen VI deficiency induces early onset myopathy in the mouse: an animal model for Bethlem myopathy. *Hum. Mol. Genet.*, **7**, 2135–2240.
41. Swaggart, K.A., Heydemann, A., Palmer, A.A. and McNally, E.M. (2011) Distinct genetic regions modify specific muscle groups in muscular dystrophy. *Physiol. Genomics*, **43**, 24–31.
42. Petrof, B.J., Shrager, J.B., Stedman, H.H., Kelly, A.M. and Sweeney, H.L. (1993) Dystrophin protects the sarcolemma from stresses developed during muscle contraction. *Proc. Natl Acad. Sci. USA*, **90**, 3710–3714.
43. Allen, D.G. (2001) Eccentric muscle damage: mechanisms of early reduction of force. *Acta Physiol. Scand.*, **171**, 311–319.
44. Blaauw, B., Agatea, L., Toniolo, L., Canato, M., Quarta, M., Dyar, K.A., Danieli-Betto, D., Betto, R., Schiaffino, S. and Reggiani, C. (2010) Eccentric contractions lead to myofibrillar dysfunction in muscular dystrophy. *J. Appl. Physiol.*, **108**, 105–111.
45. Huijing, P.A., Voermans, N.C., Baan, G.C., Buse, T.E., van Engelen, B.G. and de Haan, A. (2010) Muscle characteristics and altered myofascial force transmission in tenascin-X-deficient mice, a mouse model of Ehlers-Danlos syndrome. *J. Appl. Physiol.*, **109**, 986–995.
46. Gerrits, K.H., Voermans, N.C., de Haan, A. and van Engelen, B.G. (2013) Neuromuscular properties of the thigh muscles in patients with Ehlers-Danlos syndrome. *Muscle Nerve*, **47**, 96–104.
47. Templeton, G.H., Sweeney, H.L., Timson, B.F., Padalino, M. and Dudenhoeffer, G.A. (1988) Changes in fiber composition of soleus muscle during rat hindlimb suspension. *J. Appl. Physiol.*, **65**, 1191–1195.
48. Bigard, A.X., Boehm, E., Veksler, V., Mateo, P., Anflous, K. and Ventura-Clapier, R. (1998) Muscle unloading induces slow to fast transitions in myofibrillar but not mitochondrial properties. Relevance to skeletal muscle abnormalities in heart failure. *J. Mol. Cell. Cardiol.*, **30**, 2391–2401.
49. Ohira, Y., Yoshinaga, T., Nomura, T., Kawano, F., Ishihara, A., Nonaka, I., Roy, R.R. and Edgerton, V.R. (2002) Gravitational unloading effects on muscle fiber size, phenotype and myonuclear number. *Adv. Space Res.*, **30**, 777–781.
50. Voermans, N.C., Bonnemann, C.G., Huijing, P.A., Hamel, B.C., van Kuppevelt, T.H., de Haan, A., Schalkwijk, J., van Engelen, B.G. and Jenniskens, G.J. (2008) Clinical and molecular overlap between myopathies and inherited connective tissue diseases. *Neuromuscul. Disord.*, **18**, 843–856.
51. Abecasis, G.R., Cherny, S.S., Cookson, W.O. and Cardon, L.R. (2002) Merlin—rapid analysis of dense genetic maps using sparse gene flow trees. *Nat. Genet.*, **30**, 97–101.
52. Emsley, J., Knight, C.G., Farndale, R.W., Barnes, M.J. and Liddington, R.C. (2000) Structural basis of collagen recognition by integrin alpha2beta1. *Cell*, **101**, 47–56.
53. Mathur, A., Shankaracharya, and Vidyarthi, A.S. (2011) SWIFT MODELLER v2.0: a platform-independent GUI for homology modeling. *J. Mol. Model.*, **18**, 3021–3023.
54. Schwede, T., Kopp, J., Guex, N. and Peitsch, M.C. (2003) SWISS-MODEL: an automated protein homology-modeling server. *Nucleic Acids Res.*, **31**, 3381–3385.
55. Brünger, A.T., Adams, P.D., Clore, G.M., DeLano, W.L., Gros, P., Grosse-Kunstleve, R.W., Jiang, J.S., Kuszewski, J., Nilges, M., Pannu, N.S. *et al.* (1998) Crystallography & NMR system: a new software suite for macromolecular structure determination. *Acta Crystallogr. D Biol. Crystallogr.*, **54**, 905–921.
56. Van Der Spoel, D., Lindahl, E., Hess, B., Groenhof, G., Mark, A.E. and Berendsen, H.J. (2005) GROMACS: fast, flexible, and free. *J. Comput. Chem.*, **26**, 1701–1718.
57. Bayer, M.L., Yeung, C.Y., Kadler, K.E., Qvortrup, K., Baar, K., Svensson, R.B., Magnusson, S.P., Krogsgaard, M., Koch, M. and Kjaer, M. (2010) The initiation of embryonic-like collagen fibrillogenesis by adult human tendon fibroblasts when cultured under tension. *Biomaterials*, **31**, 4889–4897.
58. Tillet, E., Wiedemann, H., Golbik, R., Pan, T.C., Zhang, R.Z., Mann, K., Chu, M.L. and Timpl, R. (1994) Recombinant expression and structural and binding properties of alpha 1(VI) and alpha 2(VI) chains of human collagen type VI [published erratum appears in Eur J Biochem 1994 Jun 15;222(3):1064]. *Eur. J. Biochem.*, **221**, 177–185.
59. Schmittgen, T.D. and Livak, K.J. (2008) Analyzing real-time PCR data by the comparative C(T) method. *Nat. Protoc.*, **3**, 1101–1108.
60. Birk, D.E. and Trelstad, R.L. (1986) Extracellular compartments in tendon morphogenesis: collagen fibril, bundle, and macroaggregate formation. *J. Cell Biol.*, **103**, 231–240.
61. Selsby, J., Pendrak, K., Zadel, M., Tian, Z., Pham, J., Carver, T., Acosta, P., Barton, E. and Sweeney, H.L. (2010) Leupeptin-based inhibitors do not improve the mdx phenotype. *Am. J. Physiol. Regul. Integr. Comp. Physiol.*, **299**, R1192–R1201.
62. Selsby, J.T., Morine, K.J., Pendrak, K., Barton, E.R. and Sweeney, H.L. (2012) Rescue of dystrophic skeletal muscle by PGC-1α involves a fast to slow fiber type shift in the mdx mouse. *PLoS ONE*, **7**, e30063.
63. Moorwood, C., Liu, M., Tian, Z. and Barton, E.R. (2013) Isometric and eccentric force generation assessment of skeletal muscles isolated from murine models of muscular dystrophies. *J. Vis. Exp.*, **71**, e50036.